A novel concept for analysis and performance evaluation of wheeled rovers

Bahareh Ghotbi, Francisco González, József Kövecses, Jorge Angeles

This is a post-peer-review, pre-copyedit version of an article published in Mechanism and Machine Theory. The final authenticated version is available online at: https://doi.org/10.1016/j.mechmachtheory.2014.08.017.

Abstract

The analysis, design and operation planning of rovers are often based on predictive dynamic simulation, where the multibody model of the vehicle is combined with terramechanics relations for the representation of the wheel-ground interaction. There are, however, limitations in terramechanics models that prevent their use in parametric analysis and simulation studies.

Increasing mobility is generally a primary objective for the design and operation of rovers. The models and assumptions used in the analysis phase should target this objective. In this paper we put forward a new concept for the analysis of wheeled rovers, particularly for applications in off-road environments on soft soil. We propose a novel view of the problem based on the development of models that are primarily intended to represent how parameter changes in the robot design can influence performance. These models allow for the definition of indicators, which gives information about the behaviour of the system. We term such models *observative*.

In the reported work, a set of indicators for rover performance are formulated using such models. The ability of these indicators to characterize the behaviour of a rover is assessed with a series of simulation tests and experiments. The indicators defined using observative models succeeded to capture the changes in rover performance due to variations in the system parameters. Results show that the proposed models can provide a useful tool for the design and operation of planetary exploration rovers.

Keywords: Wheeled mobile robots, planetary exploration rovers, terramechanics models, terrain interaction, observative models.

1 Introduction

Mobile robots are among the best candidates for planetary surface exploration, due to their good performance in unstructured environments. Predictive dynamic simulation of mobile robots aims to anticipate the time response of the system and the representative forces as close to the real-life physical system as possible. Simulation includes the solution of an initial value problem of the governing dynamic equations. The mathematical model that forms the basis of such simulation studies must include all elements of the system as close to reality as possible. This is an extremely challenging task. The most problematic element is usually the wheel-soil interaction. The detailed study of the latter, known as terramechanics, plays a key role in the design, analysis and simulation of wheeled mobile robots; significant advances have been made during recent years in this field [9, 8]. Nonetheless, there are many open issues that can be mentioned. For example, robots are required to be robust to environmental uncertainties when it comes to semi-autonomous missions. However, terramechanics models can be very sensitive to the inaccuracies in the soil parameters [10]; the identification of these parameters is a major challenge [14]. Also, the fidelity of the terramechanics models can be questioned. The detailed modelling of the vehicle-terrain interaction may not be able to provide high-fidelity estimation of the forces involved in the interaction. The models are even less accurate when exact information on terrain properties is not available, which is particularly the case for planetary-exploration rovers. Conventional terramechanics models, e.g. those of Bekker and Wong [6, 24], have not really been developed for application in dynamic analysis and simulation. Furthermore, these models do not provide a full insight on how the variations of the system parameters can influence the reaction forces and performance. This is the motivation for proposing a new concept to capture the representative aspects of the behaviour of the physical system, those that are important for performance evaluation and can result in parametric models for design analysis.

The experience of recent planetary exploration missions has brought to the limelight many challenges that must be faced in the autonomous operation of mobile robots in unstructured environments; these involve interaction with soft terrain and sloped and rocky surfaces. Which brings the need for simulation and analysis tools that should provide a way of characterizing

the mobility of the system under various terrain conditions. Recent efforts in this area have led to the development of several simulation toolboxes that include multibody dynamics models of mobile robots and wheel-soil interaction models. ROAMS [18] is a physics-based simulator that considers mechanical and electrical subsystems of robotic systems as well as vehicle-terrain interactions. Some other examples of simulation tools developed for performance optimization and chassis analysis are POT [22] and RCAST [5]. The analysis results provided by these simulation toolboxes can be useful in evaluating different design ideas and control strategies [20].

Rover performance can be analyzed considering different aspects. One of them is mobility, which is specially important in applications on unknown and soft terrain. Due to the autonomous nature of planetary applications, it is critical to identify possible strategies to enhance the mobility of the rover and the modes of failure. Mobility is not rigorously defined in the literature for wheeled vehicles operating on soft soil. The concept is clearly defined for mechanism models where the connections between the links are given with holonomic or nonholonomic kinematic constraints, e.g. for linkages or wheeled robots operating on hard surfaces [7]. However, for rovers operating on soft terrain, generally such kinematic constraints cannot be given a priori for the modelling of wheel-ground interaction. Also, for wheeled rovers mobility is often meant in a different sense: *the ability to move from a certain configuration or to move with maximum speed.* Apostolopoulos [1] categorized the mobility performance of wheeled robots under three terms: *maneuverability*, *terrainability*, and *trafficability*. Maneuverability refers to the steering capabilities of the robot and its ability to navigate through obstacles in cluttered environments. Based on this definition, locomotion parameters such as the robot length to width ratio can then be calculated as functions of traction forces and total motion resistance developed at the wheel-terrain contact. Terrainability is the ability to negotiate uneven terrain without losing stability, while providing enough traction for forward motion. A parametric relation between the maximum slope the robot can climb and stability requirements, traction-force limits, and power limitations of the robot is obtained. Trafficability is defined as the ability of the robot to generate traction and overcome resistance, which is the primary focus in the context of robot mobility. In [1], the dependency of sinkage, soil traction, and motion resistance forces on wheel parameters, diameter and width, are represented by parametric expressions. All of the above expressions are obtained based on assumptions such as uniform normal stress distribution, which greatly simplifies the terramechanics relations. Some of the existing mobility indicators were studied along with novel concepts to quantify mobility, as proposed and applied to exploration rovers on hard ground [23]. These indices include minimum friction requirement at wheel-ground contact for

forward motion, maximum actuation torque requirement, total slip distance over the course of a run, and average violation of pure rolling constraint among all wheels of the vehicle. In fact, slip plays a key role in the determination of the mobility of a wheeled rover on soft soil, as pure rolling cannot always be guaranteed during motion. Moreover, Iagnemma et al. [16] showed that using simulation results, due to the slip-sinkage effect, increased slippage causes additional sinkage of the wheel, which will result in increased motion resistance. The concept of maximum mobility for wheeled robots on soft soil is thus related to minimizing the slip of the wheels.

In order to improve the behaviour of a rover it is necessary to identify the influential parameters at the design and operation levels. In different designs of planetary rovers the parameters that can be tuned during the operation vary. In some designs it is possible to control the distribution of input power among the wheels. In several studies [13, 21, 19] improvement of the wheel traction through proper selection of input torques to the wheels is discussed. Lamon et al. considered quasi-static modelling, as the dynamic effects are assumed to be negligible within the range of robot speed, while the calculation of the friction requirement is based on the Coulomb friction model [19]. However, in practice, the value of the friction coefficient is not known. According to the foregoing approach it is first assumed that the wheel does not slip and the ratio of traction to normal force falls below the actual friction coefficient. With this assumption it is possible to calculate normal and traction forces as functions of torque applied to the wheel. Next, in an optimization process an input torque that minimizes the ratio of traction to normal force is calculated. By doing this, the chance that this ratio be smaller than the friction coefficient increases.

Previous work by the authors showed that similar simplified models can generally be used to characterize the behaviour of the system [11]. Such models are not intended to replace their terramechanics counterparts. However, they can be used to predict the way in which a change in the design, actuation or configuration of the rover will affect its ability to operate. At the design and control stages it is very important to foresee all the challenging situations in which the rover would face mobility problems, to provide tools and algorithms to avoid those situations or to overcome them. In reconfigurable robots it is possible, for instance, to change the position of the centre of mass (COM) and other effective inertial properties, which can provide an important means to improve the mobility of the system and its stability [15]. The effect of changes in other parameters such as distribution of input torque and wheel radius is also discussed in this paper.

2 Dynamics modelling

2.1 General formulation

A key element in wheeled mobile robots is the characterization of their interaction with the ground via the wheels. The wheel-ground contact usually involves a complex geometry and a finite contact area. However, the forces exchanged between wheel and ground can generally be represented with a resultant force and a resultant moment about a reference point on the perimeter of the wheel. Based on this we will assume that the contact forces will be represented this way with a reference *contact point*.

If the rover is freed from the contact with the ground, then its configuration can be represented with a minimum set of n generalized coordinates arrayed in vector $\mathbf{q}$.[1] Using this set of coordinates for the parametrization of the dynamics, the model of the rover can be expressed as

$$\mathbf{M}\ddot{\mathbf{q}} + \mathbf{c} = \mathbf{f} \tag{1}$$

where $\mathbf{M}$ is the $n \times n$ mass matrix of the system, $\mathbf{c}$ the n dimensional array of Coriolis and centrifugal terms, and $\mathbf{f}$ the n dimensional array of generalized forces. The generalized forces include three main parts: $\mathbf{f} = \mathbf{f}_w + \mathbf{f}_d + \mathbf{f}_o$, where $\mathbf{f}_w$ represents the wheel-ground interactions, $\mathbf{f}_d$ is associated with the desired rover motion, and $\mathbf{f}_o$ represents the other loads acting on the system, e.g. gravity.

In the general case, the kinematic relations that describe the motion of the wheels in contact with the ground are non-holonomic. At the velocity level they can be written as

$$\mathbf{A}\dot{\mathbf{q}} - \mathbf{s} = \mathbf{0} \tag{2}$$

where $\mathbf{A}$ is the $m \times n$ matrix representing the expression of the velocities of the wheel-contact points and frames in terms of the selected generalized velocities, and $\mathbf{s}$ the m dimensional array of the velocities of the wheel contact points and frames; this includes, for example, wheel slip and also the possible motion of the wheel in a direction normal to the ground. This velocity-level

[1] We note that the selection of this set of coordinates is not unique; the choice of coordinates depends on the analyst, the system, and the need at hand.

relationship can also be expressed at the acceleration level as

$$\mathbf{A}\ddot{\mathbf{q}} + \dot{\mathbf{A}}\dot{\mathbf{q}} - \dot{\mathbf{s}} = \mathbf{0} \tag{3}$$

The required motion of the rover can be represented by a set of p kinematic relations. For instance, it is possible to specify the desired forward acceleration or velocity of the rover for a given manoeuvre. If these relations are holonomic, they can be expressed at the configuration level as $\mathbf{\Phi}_d(\mathbf{q}, t) = \mathbf{0}$. Their corresponding velocity-level expression is in the form

$$\mathbf{B}\dot{\mathbf{q}} - \mathbf{b} = \mathbf{0} \tag{4}$$

where $\mathbf{B}$ is the $p \times n$ matrix that represents the required rover motion in terms of the generalized velocities, and $\mathbf{b} = \mathbf{b}(t)$ is the p dimensional array of required rover velocities. At the acceleration level these relations can be written as

$$\mathbf{B}\ddot{\mathbf{q}} + \dot{\mathbf{B}}\dot{\mathbf{q}} - \dot{\mathbf{b}} = \mathbf{0} \tag{5}$$

Based on the kinematic relations given by Eqs. (2) and (4) the decomposition of the generalized forces in Eq. (1) can be represented in more detail as

$$\mathbf{f} = \underbrace{\mathbf{A}^{\mathrm{T}}\boldsymbol{\lambda}_w}_{\mathbf{f}_w} + \underbrace{\mathbf{B}^{\mathrm{T}}\boldsymbol{\lambda}_d}_{\mathbf{f}_d} + \mathbf{f}_o \tag{6}$$

where $\boldsymbol{\lambda}_w$ is the m dimensional array of ground reactions transmitted to the wheels from the ground, and $\boldsymbol{\lambda}_d$ is the p dimensional array that represents the generalized forces associated with the p required rover motion specifications. Henceforth, we will assume that either the required rover motion is specified via $\mathbf{b}$ and Eqs. (5) and (4), or the forces and moments $\boldsymbol{\lambda}_d$ associated with these kinematic constraints are given directly.

In the case of rovers operating on unstructured terrain, the nature of the wheel-ground interaction presents a significant, additional difficulty. The task of the analyst is to choose the most suitable interaction model to describe the representative phenomenon. This can generally be done in two different ways, either by specifying the forces and moments $\boldsymbol{\lambda}_w$ developed at the wheel-ground contacts via constitutive relations, or imposing representative kinematic specifications on the wheel-ground interface motions represented by $\mathbf{s}$ in the model above. We will

consider two representative cases here.

2.2 Operation on hard terrain

This is the most common case considered for wheeled robots in the literature. For these operations it can generally be a reasonable approach to assume that the wheel-ground interaction can be well-represented by *kinematic specifications*, namely, the conditions of no slip and no penetration. In the formulation presented above this is represented by imposing the kinematic constraints $\mathbf{s} = \mathbf{0}$. With this the ground reactions $\boldsymbol{\lambda}_w$ will become generalized constraint forces, i.e. part of the variables that are determined by the system dynamics.

2.3 Operation on soft terrain

For this situation the kinematic specifications of no slip and no penetration are generally not applicable; a better characterization of the wheel-ground interaction can be achieved by means of constitutive relations. These can be based on the terramechanics relations proposed by Bekker [6], later modified by Wong and Reece [24], which are the most widely used relations for wheel-terrain interaction on soft soil. They offer a relatively good approximation for the case of steady-state motion. However, there can be many problems with the application of these formulas, particularly due to the highly uncertain parameters that need to be identified with extensive experimental work; however, the results of the identification task can be highly sensitive to changes of soil or environmental conditions. Also, these formulas may fail to provide proper representations for dynamic operating conditions. Several new terramechanics models have also been developed based on the concepts put forth by Bekker [6] and Wong [24]. These also suffer from several of the above-mentioned shortcomings, yet this classical terramechanics approach still provides the simplest state-of-the-art representation to develop constitutive relations of the wheel-ground interaction on soft soil.

In the Bekker and Wong models [6, 24] the terrain reaction forces are obtained by integrating the normal stress σ and the shear stress τ over the wheel contact area. This gives the elements of $\boldsymbol{\lambda}_w$ for each individual wheel. Figure 1 shows the interpretation of these force and moment components as well as the representative wheel parameters and variables. According to this

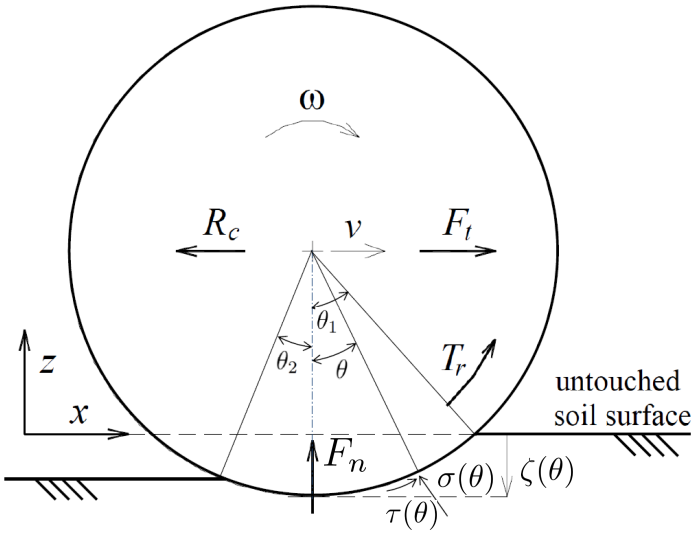

Figure 1: Free-body diagram of a rigid wheel in contact with soft soil

figure, in the x-direction, parallel to the soil surface, the reaction force R_c opposes the motion, while F_t is the tangential, traction force component. For the normal direction, F_n represents the normal reaction and T_r the resisting torque about the axis of the wheel. Based on [6] and [24], and also considering the modifications proposed in [3] the expressions for these components can be derived as

$$R_c = rb \int_{\theta_2}^{\theta_1} \sigma(\theta) \sin\theta d\theta, \tag{7}$$

$$F_t = rb \int_{\theta_2}^{\theta_1} \tau(\theta) \cos\theta d\theta, \tag{8}$$

$$F_n = rb \int_{\theta_2}^{\theta_1} [\tau(\theta) \sin\theta + \sigma(\theta) \cos\theta] d\theta - c_z \dot{z}, \tag{9}$$

$$T_r = r^2 b \int_{\theta_2}^{\theta_1} \tau(\theta) d\theta \tag{10}$$

In the above relations, r and b are the wheel radius and width, respectively, θ_1 and θ_2 indicating the angles associated with the beginning and end points of contact on the wheel perimeter. In the Bekker model, θ_2 is zero. The term $c_z\dot{z}$ in Eq. (9) introduces a state-dependent damping [3], with $\dot{z}$ denoting the velocity of the wheel centre in the normal direction.

In Eqs. (7) – (10), the normal stress at the wheel-terrain interface is given by:

$$\sigma(\theta) = \left(\frac{k_c}{b} + k_\phi\right) \zeta(\theta)^n \tag{11}$$

where n is the sinkage exponent, ζ is the vertical sinkage at any point on the contact surface, and k_c and k_ϕ denote the pressure-sinkage moduli associated with the soil cohesive and frictional components, respectively. The shear stress can be determined as

$$\tau(\theta) = [c + \sigma(\theta)\tan\phi]\left[1 - e^{\frac{-r}{K_d}[\theta_1 - \theta - (1-i)(\sin\theta_1 - \sin\theta)]}\right] \tag{12}$$

where c is the terrain cohesion, ϕ is the internal friction angle, K_d is the shear deformation modulus, and i is the wheel slip ratio, defined as $i = (r\omega - v)/r\omega$. In Eqs. (11) and (12), n, k_c, k_ϕ, c, ϕ, and K_d are terrain parameters that need to be determined experimentally.

The forces and moments in Eqs. (7)–(10) represent the soil reactions developed in the plane defined by the wheel and resolved about the wheel centre point. This is the form typically used in terramechanics. To obtain the resultant components that form the elements of $\boldsymbol{\lambda}_w$ this system of forces needs to be interpreted in terms of the representative contact point of the wheel. These components can be obtained via a simple transformation. Additionally, soil reactions perpendicular to the plane of the wheel, such as lateral bulldozing forces [17], can also contribute to the elements of $\boldsymbol{\lambda}_w$.

The modifications introduced by Azimi et al. [3] were particularly concerned with the motion in the normal direction. The use of the original terramechanics formulas for dynamic operating conditions would result in unrealistic, undamped oscillations in the normal direction. The reason is that the normal pressure-vs.-sinkage curve determined via the bevameter tests [6, 24] may be seen as the constitutive relation of a nonlinear spring, which would certainly not be representative of dynamic wheel-ground interactions when the soil behaves as an elasto-plastic medium. The modification introduced in [3] involves a dissipative term for motion in the normal direction to better reflect what can be observed in reality. This term has no effect under steady-state conditions, which imply zero rate of sinkage, for which the classical terramechanics formulas provide reasonable representations. However, this additional term extends the usability and applicability of the formulas for dynamic operating conditions. These have been illustrated with simulation and experiments [2]. Alternative wheel-terrain interaction models have been recently introduced in the literature, e.g. [4], which intend to provide a more accurate representation of the phenomena at the contact interface. These include damping in a more natural way, in the constitutive model of the wheel-soil interaction.

As mentioned above, the terramechanics representations are highly sensitive to the soil pa-

rameters. The sensitivity of the dynamic response of a single wheel to small changes in some soil parameters, such as the friction angle and the apparent cohesion coefficient was studied in [10]. It was shown that the dynamic response is usually extremely sensitive to even small changes in soil parameters, as completely different results can be obtained with small perturbations in the parameters. This also points to the need of exploring alternative possibilities for the analysis of rovers operating on soft soil.

3 Observative models for analysis

In the two cases discussed above, the intention generally is to approximate the key phenomena of wheel-ground interaction as closely as possible with the selection of the appropriate model and point of view. For hard terrain this can be achieved by representing the interaction using kinematic specifications in the first place; for soft terrain, the representation of the interaction forces via constitutive relations seems usually the appropriate choice. However, the development of the appropriate constitutive relations for the wheel-soil interaction is an extremely challenging task; no model is available currently that would be able to address a broad range of operating conditions with high-enough fidelity.

On the other hand, the dynamics formulation described in Subsection 2.1 allows for the development of an alternative point of view in the analysis of rovers on soft soil. This relates to the definition of conditions that can contribute to the increase in rover mobility; the reformulation of the dynamics model with the appropriate selection of base variables reflects how parametric changes in the system affect the desired optimum conditions. We term such models *observative*, as the general intention and point of view are different compared to the traditional developments of predictive dynamic simulations where high fidelity soil modelling is an essential aspect. In the observative point of view we rather try to eliminate the detailed constitutive modelling of the soil via formulating the appropriate conditions for mobility improvement and performance indicators based on those.

We conjecture that maximum mobility for a rover moving straight is achieved when the wheel slip is zero[2]. We define a zero wheel-slip when the instant centre of velocity of the wheel

[2]If a rover is turning, then mobility also depends on the type of steering concept used.

relative to the inertial, ground-fixed frame is the contact point, defined earlier, that is on the characteristic perimeter of the wheel.[3] In such a case the velocity of the centre of the wheel and its angular velocity are connected via velocity-level kinematic relationships, which are the same type as the ones appearing for hard terrain contact representation. Some elements of the $\mathbf{s}$ and $\dot{\mathbf{s}}$ arrays in Eqs. (3) and (2) are specified as zero. This concept can be generalized for slip values different from zero also. In the case of zero slip the main body of the rover can achieve maximum speed. The question is how this maximum mobility can be accomplished, and how the system parameters affect that.

Most investigations based on dynamic simulation focus on what is known as the drawbar pull as a measure to characterize system mobility. The drawbar pull is related to the traction forces developed by the wheels and the ability of the rover to pull a load. The maximum drawbar pull is usually observed at nonzero slip ratios, depending on the soil and wheel properties [24].

However, it is noteworthy that drawbar pull is not directly related to the mobility of the system. The drawbar pull is not a representative measure of the ability of the rover to attain maximum mobility. We also conjecture that the motion with maximum mobility is a natural motion of the system, i.e. it moves as such unless the conditions and connections to its environment cannot make that possible. When the rover is moving, actuation is applied on certain wheels, and the contact between wheel and ground is necessary to propel the vehicle. On the other hand, this contact is passive and the reaction force between wheel and ground is *developed*, not *applied*, which is a very important point. Only as much reaction force is developed as needed to achieve the maximum mobility. In other words, the wheels only slip when they have to. For example, it can be observed with off-road vehicles and rovers that considerable slip is not necessarily developed when the terrain is able to provide enough traction. In this case, the vehicle achieves maximum mobility. The level of reaction force needed to maintain the maximum mobility condition depends on the rover design and loading. The transition from maximum mobility to lower mobility occurs when the wheel-ground interface cannot develop the necessary reaction force anymore. In such a case the wheel starts to slip in order to accommodate the increased load, which decreases mobility, i.e. the instant velocity centre of the wheel with respect to the unperturbed, fixed ground tends to move closer to the wheel centre. The same reasoning can

[3] At every instant the wheel geometry naturally defines a plane; the wheel motion can be decomposed into motion parallel to this plane and motion perpendicular to that. The general definition of the instant centre relates to the part of the wheel motion that is parallel to the reference plane.

apply to wheel motions normal to the ground: the wheel only sinks as much as needed for the terrain to develop the necessary reaction forces.

From the point of view of energy considerations, the desired situation, in which wheel slip and sinkage are zero, is also the most efficient mode of operation. In that case, all the power applied to the wheel is spent on accelerating the system, i.e., in increasing its kinetic energy. If slip and sinkage are present, a fraction of the input power is always dissipated.

Considering the dynamics formulation presented in Section 2.1 we can consider two situations. In the first, the forces and moments $\boldsymbol{\lambda}_d$ associated with the required rover motion are explicitly given, and Eqs. (5) and (4) do not apply. Then, based on the rest of Eqs. (1) – (6) the wheel-ground interaction forces and moments can be expressed as

$$\boldsymbol{\lambda}_w = (\mathbf{A}\mathbf{M}^{-1}\mathbf{A}^{\mathrm{T}})^{-1}\left[\mathbf{A}\mathbf{M}^{-1}\left(\mathbf{c} - \mathbf{B}^{\mathrm{T}}\boldsymbol{\lambda}_d - \mathbf{f}_o\right) - \dot{\mathbf{A}}\dot{\mathbf{q}} + \dot{\mathbf{s}}\right] \tag{13}$$

In the second case, the kinematic specifications associated with the required rover motion are given as per Eqs. (5) and (4). In this case, the problem can be cast in a more compact form if the definitions below are introduced:

$$\mathbf{D} = \begin{bmatrix} \mathbf{A} \\ \mathbf{B} \end{bmatrix} \; ; \quad \mathbf{d} = \begin{bmatrix} \mathbf{s} \\ \mathbf{b} \end{bmatrix} \; ; \quad \boldsymbol{\lambda} = \begin{bmatrix} \boldsymbol{\lambda}_w \\ \boldsymbol{\lambda}_d \end{bmatrix} \tag{14}$$

With these definitions the dynamics and kinematics equations of (1) – (6) can be rewritten as

$$\mathbf{M}\ddot{\mathbf{q}} + \mathbf{c} = \mathbf{D}^{\mathrm{T}}\boldsymbol{\lambda} + \mathbf{f}_o \tag{15}$$

$$\mathbf{D}\ddot{\mathbf{q}} + \dot{\mathbf{D}}\dot{\mathbf{q}} - \dot{\mathbf{d}} = \mathbf{0} \tag{16}$$

and

$$\mathbf{D}\dot{\mathbf{q}} - \mathbf{d} = \mathbf{0} \tag{17}$$

In this case, $\boldsymbol{\lambda}$ turns out to be

$$\boldsymbol{\lambda} = (\mathbf{D}\mathbf{M}^{-1}\mathbf{D}^{\mathrm{T}})^{-1}\left[\mathbf{D}\mathbf{M}^{-1}\left(\mathbf{c} - \mathbf{f}_o\right) - \dot{\mathbf{D}}\dot{\mathbf{q}} + \dot{\mathbf{d}}\right] \tag{18}$$

Hence, the wheel-ground interaction reaction representations can be obtained as the first m

entries of $\boldsymbol{\lambda}$

$$\boldsymbol{\lambda}_w = \boldsymbol{\lambda}_{(1:m)} \tag{19}$$

These expressions open up a broad range of possibilities for parametric analyses[4]. We can see that Eqs. (13) and (19) give the expression of the wheel-ground reactions as a function of the rover system parameters, the desired operation of the rover, and the kinematics and the wheel-ground interfaces, e.g., slip and sinkage. In the observative model concept, these force representations can play the role of primary variables to characterize the vehicle-terrain interaction behaviour with respect to changes in the parameters and the state of the rover.

If we employ conditions for maximum mobility or requirements for sinkage, then some or all of the entries of $\mathbf{s}$ are given. The above formulas give the required terrain reactions to maintain the specified operating conditions. For example, the transition from maximum mobility to lower mobility occurs when the wheel-ground interface cannot develop the necessary reaction force anymore without slipping. In such a case the wheel starts to slip to accommodate the increased load and the mobility decreases, i.e. the instant velocity centre of the wheel tends to move closer to its axis. The form of Eqs. (13) and (19) allows one to conduct a parametric study that can provide useful information on where the transition from higher mobility to lower mobility takes place and which rover parameters affect that. This representation allows the analyst to study how the rover design and control parameters can influence this transition. The analysis of how changes in rover parameters can reduce the necessary level of reaction force to maintain the required conditions can help achieve better performance. Regardless of the soil characteristics, if lower tangential reaction forces are required for a manoeuvre, then that would give the vehicle a higher chance of maintaining the no-slip condition. The tangential reaction force components in $\boldsymbol{\lambda}_w$, associated with the slip specifications, can be considered as one set of the performance indicators used to characterize the effect of changes in rover parameters on the contact interface behaviour and mobility.

On the other hand, the distribution of the normal reaction force components, also present in $\boldsymbol{\lambda}_w$, may also have an immediate influence on the mobility and performance of a rover. These normal reactions can directly influence the maximum tangential reaction forces that can be

[4]We note that for the above formulas it is assumed that both $\mathbf{A}$ and $\mathbf{D}$ have full row rank; in other words all kinematic relations are independent of each other. For systems where this assumption is not valid, the methods reported in [12] can be used to determine $\boldsymbol{\lambda}$ and $\boldsymbol{\lambda}_w$.

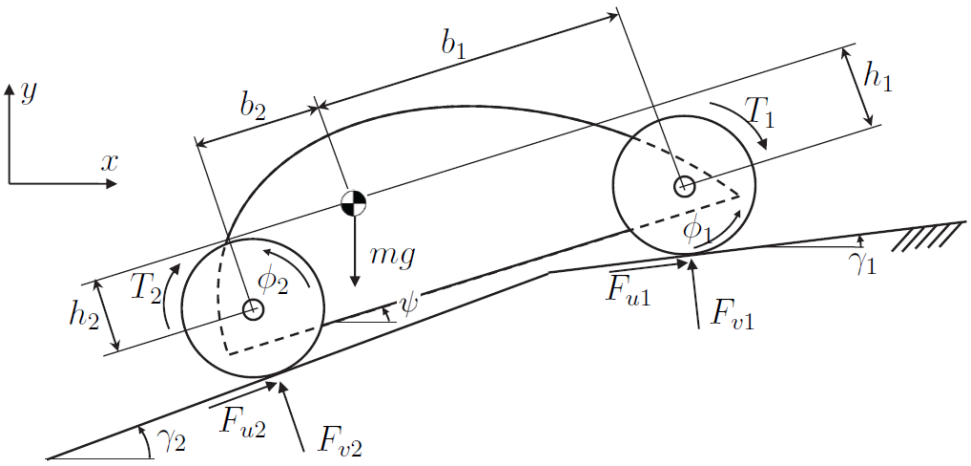

Figure 2: A 5 degree-of-freedom, 2-D model of a planetary rover on uneven terrain

developed at the wheel-ground interfaces. This is also supported by general terramechanics observations [24], which can bring about the possibility to develop a performance indicator based on the distribution of the normal reaction forces. These forces can also be important for stability analysis [21]. The ratio of tangential to normal force as a function of rover parameters can be used in optimization procedures to reduce the chance of slip and achieve desired values [19].

4 Illustration with simulation

A two-dimensional, five degree-of-freedom multibody model of a rover, illustrated in Fig. 2, is used in this section. In the dynamics model of the vehicle the generalized coordinates are the Cartesian coordinates of the centre of mass (COM) of the vehicle, x_G and y_G, the rotation ψ of the body with respect to the x axis, and the rotation of the front and rear wheels with respect to the vehicle main frame, ϕ_1 and ϕ_2. Parameters b_i and h_i represent the distance of the COM to the centre of the i^{th} wheel, for $i = 1, 2$. The mass of the vehicle body is m_b and its moment of inertia about the axis normal to the plane is I_b. The mass and radius of wheel i are m_i and r_i, respectively. The moment of inertia of wheel i about its axis, assumed to pass through the wheel COM, is given by I_i.

The input torques applied to the wheels are T_1 and T_2; they are related to each other with a proportionality ratio α as $T_2 = \alpha T_1$. The wheel-terrain interaction forces in the tangential and normal directions of the contact for wheel i are F_{ui} and F_{vi} respectively. The contact between

ground and wheels can be considered in two alternative ways, as described below.

4.1 Predictive model

A predictive model of the rover can be developed using the terramechanics relations in Eqs. (7)–(10). These relations are based on [6] and [24] and the modifications proposed in [3]. The wheel-terrain interaction forces $\mathbf{f}_w$ required by Eq. (1) are determined using this predictive model.

The tangential and normal components of interaction are

$$F_{ui} = F_{ti} - R_{ci} \tag{20}$$

$$F_{vi} = F_{ni} \tag{21}$$

As no constraint equations are imposed on the system, its number of degrees of freedom is kept as five. This model aims to provide realistic interaction forces; it can only be used in a forward-dynamics setting because Eqs. (7)–(10) evaluate these forces as functions of the configuration and velocity of the system.

4.2 Observative model

An alternative approach lies in specifying the relative motion of the wheels with respect to the ground using the kinematic mapping of Eq. (2). In this case, array $\mathbf{s}$ contains the tangential and normal components of the velocity of the application point of each contact force, and array $\boldsymbol{\lambda}_w$ contains the wheel-terrain reactions λ_{ui} and λ_{vi} required to maintain the kinematic specifications. The generalized forces representing the wheel-terrain interaction are obtained as $\mathbf{f}_w = \mathbf{A}^{\mathrm{T}}\boldsymbol{\lambda}_w$. This kinematic mapping can be used to impose no-slip and no-penetration specifications by setting $\mathbf{s} = \mathbf{0}$. This is equivalent to requiring that the velocity of the points of the wheels in contact with the terrain be zero, thus resulting in the introduction of two kinematic constraints per wheel. Consequently, the number of degrees of freedom of the system is reduced to unity. The model thus obtained can be categorized as an observative model, as introduced in Section 3.

For the case of flat terrain ($\gamma_1 = 0, \gamma_2 = 0$), the constraint reaction forces can be expressed as functions of the specified forward acceleration of the rover ($\ddot{x}_G$) and the design and operation parameters, namely,

$$\lambda_{u1} = \frac{1}{\alpha+1}\left[m_b + 2m_w - \frac{\alpha I_w}{r^2} + \frac{I_w}{r^2}\right]\ddot{x}_G \tag{22}$$

$$\lambda_{u2} = \frac{1}{\alpha+1}\left[\alpha\left(m_b + 2m_w\right) + \frac{\alpha I_w}{r^2} - \frac{I_w}{r^2}\right]\ddot{x}_G \tag{23}$$

$$\lambda_{v1} = \frac{1}{b_1+b_2}\left[-\left(m_b h + 2m_w r + m_b r\right)\ddot{x}_G - m_w g\left(b_1+b_2\right) - m_b g b_2 - 2\frac{I_w}{r}\ddot{x}_G\right] \tag{24}$$

$$\lambda_{v2} = \frac{1}{b_1+b_2}\left[\left(m_b h + 2m_w r + m_b r\right)\ddot{x}_G - m_w g\left(b_1+b_2\right) - m_b g b_1 + 2\frac{I_w}{r}\ddot{x}_G\right] \tag{25}$$

The reaction forces λ_{u1}, λ_{u2}, λ_{v1}, and λ_{v2} correspond to the components of $\boldsymbol{\lambda}$ in Eq. (18). The details of the derivation of Eqs. (22)–(25) can be found in Appendix A.

4.3 Simulation results

The two models described above are compared by means of simulation. The purpose of using the observative model is to capture the way in which reaction forces vary when the system parameters are modified. The trends obtained are compared to the results from the predictive model of Section 4.1. It will be shown that there is a direct relation between the actual level of slip that occurs during operation and the magnitude of the tangential reaction force the terrain must be able to develop to avoid slip. The tangential reaction force can be considered as an indicator for rover mobility. Three design and control parameters of the rover have been studied. The first parameter under study is the ratio α that characterizes the distribution of the resultant applied torque among the wheels. The wheel radius r and the displacement of the COM of the rover with respect to the geometric centre of the vehicle along its longitudinal axis are the two other design parameters to be assessed.

The effects of the variation of these parameters on the tangential reaction forces were studied in simulation when the rover moves on flat terrain. First, the wheel-terrain interaction forces F_{ui} and F_{vi} were determined using the predictive model with terramechanics relations (7)–(12) and the terrain parameters in Table 1.

Forward dynamics simulation was conducted to compute acceleration and terrain reaction

Table 1: Soil parameters used for the predictive model

n	c	ϕ	k_c	k_ϕ	K_d
-	[N/m^2]	[deg]	[N/m^{n+1}]	[kN/m^{n+2}]	[m]
1	800	37.2	1370	814	0.025

forces for given input torques applied to the wheels. The total applied torque T was distributed among the front and rear axles according to the expressions:

$$T_1 = \frac{1}{1+\alpha} T \; ; \qquad\qquad T_2 = \frac{\alpha}{1+\alpha} T \tag{26}$$

Torque T followed a trapezoidal profile starting from zero at $t = 1$ s, increased linearly with time to 11 Nm until $t = 2$ s, remained constant during the next 10 s, and then ramped down to 0 Nm over 1 s. Simulation studies showed that the vehicle reaches a constant acceleration $\ddot{x}_c$ between $t = 2.5$ s and $t = 12$ s. The tangent reaction forces during this period were evaluated using Eq. (20).

In order for the reaction forces obtained to be comparable, the predictive and observative models need to be considered for the same rover motion. Acceleration $\ddot{x}_c$ obtained with the predictive model, is consequently set to specify the desired motion of the rover for the observative model. Then, the required constraint reaction forces are evaluated using Eq. (18). For this particular rover, the tangential reaction forces can also be determined using Eqs. (22) and (23) as functions of the system parameters and the desired acceleration $\ddot{x}_c$.

First, the effect of the torque distribution parameter α was studied. The simulation procedure described above was repeated for a range of values of α and the tangential and normal forces were determined using the two models. Also, for each value of α the magnitude of the slip was calculated based on the predictive model. It was confirmed that changes in α had no significant effect on the normal forces. This is derived from the condition that both models must satisfy the dynamic equilibrium of the rover in the vertical direction, which is independent of α. However, the applied torque directly affects the force equilibrium of each wheel and, consequently, the resultant tangential reaction force. The net tangential force F_{ui} obtained with the predictive model and the tangential constraint force λ_{ui} given by the observative one are compared for different values of α in Fig. 3.

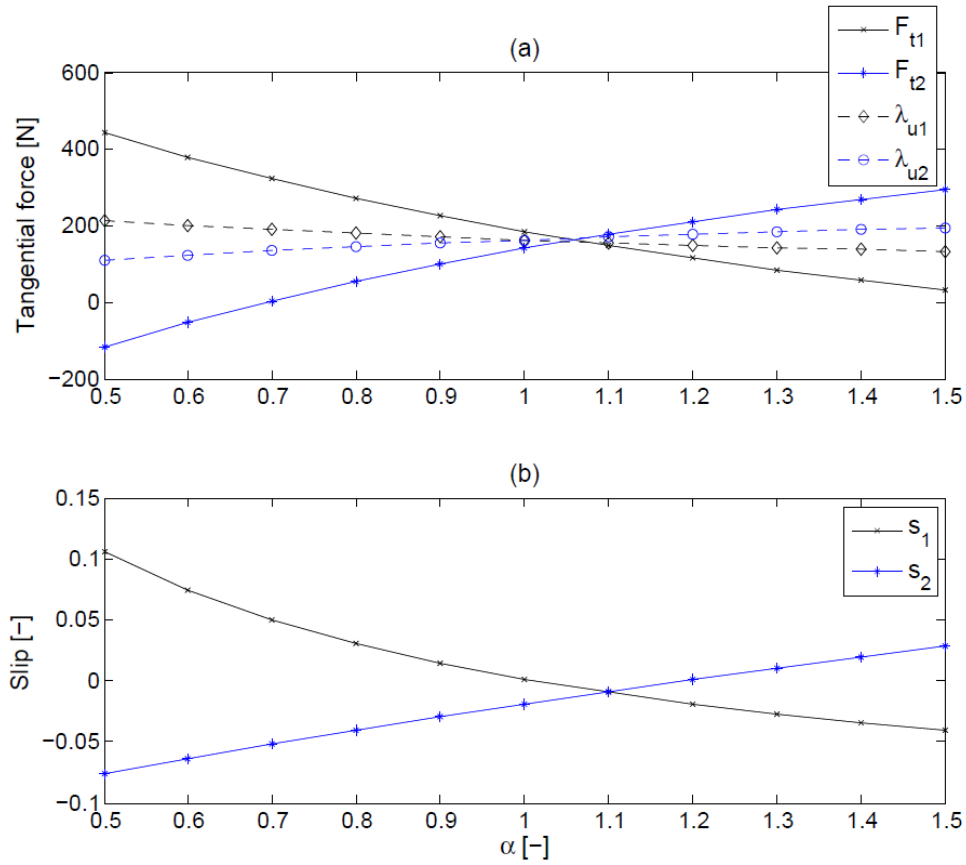

Figure 3: Effect of the variation of the torque distribution parameter α on (a) the net tangential force obtained with the observative (dashed lines) and predictive models (solid lines) and (b) the slip at the wheel-terrain contact point obtained with the predictive model

Figure 3a shows that the trends of change in the tangential forces, obtained from the predictive and observative models due to the variation of α are similar. It has to be noted that the observative model is not used here to determine the value of α for which the net traction force at the front and rear wheels is the same. It is not used either to determine the torque distribution that results in zero slip at the wheel-terrain interfaces. These values depend on the terrain characteristics and they cannot be found with the observative model. However, the change in the wheel slip due to the variation of α (Fig. 3b) does follow the same trend as the tangential reaction force. These results tally with the expectation that if the tangential forces obtained from the observative model are high, the terrain is less likely to withstand this force and the system is more prone to developing slip. The larger the constraint forces λ_{ui} are, the higher slip is to be expected in reality.

The observative model is able to indicate these effects of changes in rover parameters without the need to have a detailed representation of the soil properties. In order to investigate this in

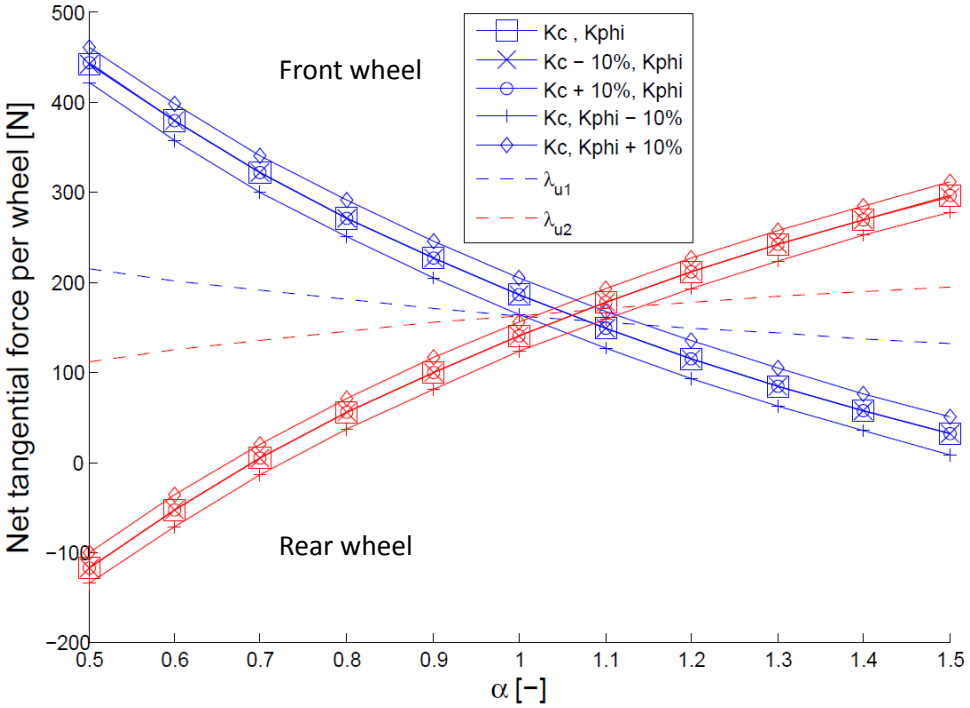

Figure 4: Effect of the variation of the torque distribution parameter α on the net tangential force obtained with the predictive model for different soil parameters (solid lines) and the observative model (dashed lines)

more detail, the simulation with the predictive model was repeated varying soil parameters k_c and k_φ from their original values given in Table 1. These parameters appear in the normal stress formula in Eq. (11). The variation of these parameters represents soils with different cohesive and frictional properties. As shown in Fig. 4, with different values of soil parameters, reaction forces obtained from terramechanics models follow the same trend as determined via the observative model.

Figure 5 shows the net tangential force developed at each wheel with the same value of the input torque, for different values of the wheel radius r. The slip developed at each wheel is important to understand this figure. It can be seen that, when using terramechanics models, larger wheels result in smaller values of the net tangential force and, consequently, in lower slip. This is to be expected, as the input torque is kept constant for different values of the wheel radius. The purpose of this study was not to find an optimum wheel radius from the point of view of rover performance, but rather to highlight that the observative model is able to capture the trends that are generally observed. Again, variations in the soil parameters do not affect the validity of the results obtained with the observative model.

The position of the centre of mass of the rover has to be also considered in the study of

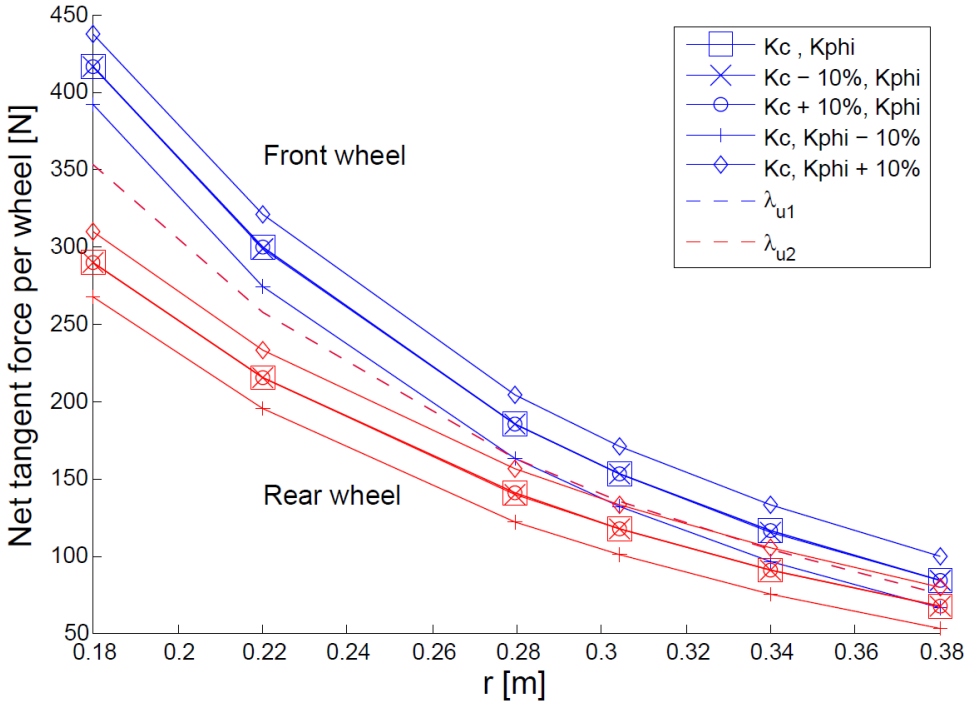

Figure 5: Effect of the variation of wheel radius on the net tangential force obtained with the predictive model for different soil parameters (solid lines) and the observative model (dashed lines), for $\alpha = 1$

mobility. Information about its effect on the performance of the system can be useful for design and operation. For the case of reconfigurable systems, for example, mass distribution can be changed while the robot is in operation in order to improve traction or stability. This reconfiguration requires knowledge of the way in which a change in configuration will influence the soil interaction.

In some cases, the study of how the COM position affects mobility can be carried out using normal forces as performance indicators. It is obvious that the change of COM position has an immediate effect on the normal force distribution among the wheels. In the case of non-redundant supporting in the normal direction, the normal forces obtained from both the predictive and observative models should be the same. Thus, without resorting to the complex and computationally expensive terramechanics relations, the mobility of a rover during operation can be studied with the aid of an observative model. The use of normal reaction forces as indicators is illustrated in Section 5 with an experimental example.

5 Experimental results

The experiments reported here were conducted on the Juno rover prototype, developed by Neptec[5], operating on soft soil, as shown in Fig. 6.

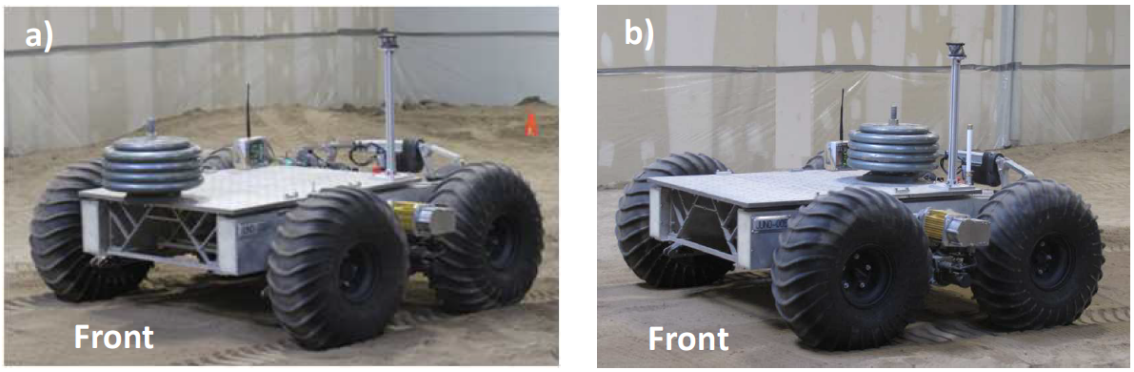

Figure 6: Juno Rover with additional mass elements in configurations A (left) and B (right)

The model of the rover can be developed in the form given previously in Section 4. The rover is instrumented with wheel encoders, inertial measurement units (IMU) and a positioning system that provides the 3-D position of the rover in global coordinates. The two wheels on each side of the rover are coupled, hence they are constrained to have the same angular velocity. Given that the distance between the two wheel centres is constant, on flat terrain they experience the same slip. Simulations using terramechanics relations described in Section 2.3 showed that, in such a case, the highest resultant traction force will be developed if the normal load distribution on the wheels is uniform. This is illustrated in Fig. 7. The plots show that when travelling on flat terrain the net tangential force obtained using the terramechanics model reaches its maximum when the normal forces experienced by the wheels are identical. This allows for using the normal force distribution as a relevant performance indicator in analyzing the mobility of this particular rover.

The load distribution can be influenced by changes in the configuration of the rover. The position of the COM resulting in a uniform normal force distribution can be found employing the observative model described in Section 4.2. Based on the equations describing the normal forces, (24) and (25), the values of parameters b_1 and b_2 that provide a uniform force distribution can be found. Given two different mass distributions for the rover, it is possible to select the one that provides larger traction forces just by comparing the normal wheel-ground reactions

[5]http://www.neptec.com

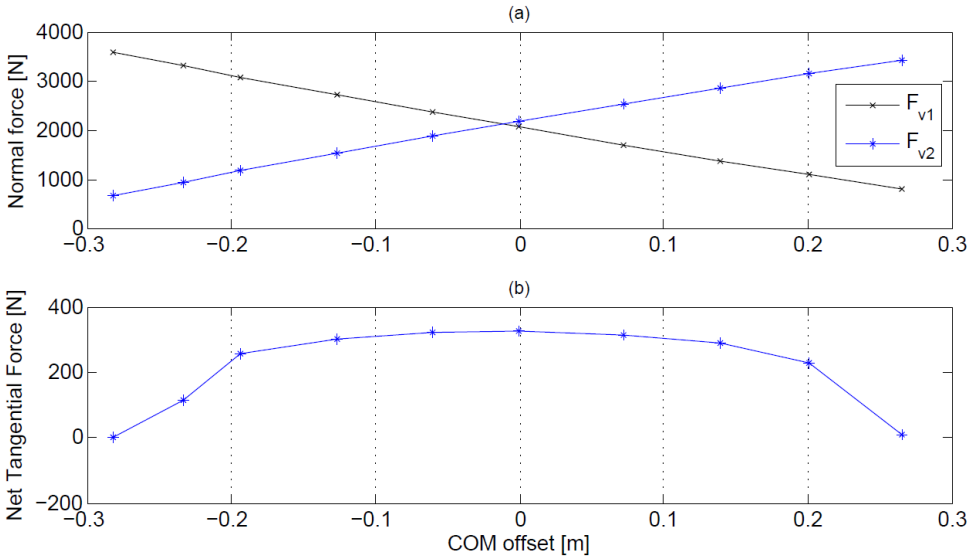

Figure 7: Effect of the COM position of the Juno rover on (a) the normal force and (b) the net tangential force at the wheel-soil interface, as predicted by simulation with Azimi et al. model [3]

evaluated with the simple observative model. To illustrate this, several different configurations of the Juno rover were compared in terms of the drawbar pull the vehicle was able to develop. The design of the platform of the Juno rover does not allow for direct geometric reconfiguration. However, as additional components, such as manipulator arms or payload, will be present in real-life missions, the configuration of these elements is bound to change the position of the COM. Therefore, in order to obtain different configurations with the same rover chassis, an additional set of mass elements was placed on different points on the rover platform, as shown in Fig. 6, making sure that the total mass was the same in all experiments.

The mass of the rover was found to be 317.5 kg; additional mass elements, including attachments, weighed a total of 111.4 kg, resulting in a total mass of 428.9 kg. Therefore, changing the position of the mass elements on the rover platform had a significant effect on the horizontal position of the COM of the overall rover system. Selected results for two positions of the additional mass are shown in Fig. 8 and analyzed next. The configuration in which the mass elements are located on the front tip of the longitudinal axis of the rover is labelled A (Fig. 6a). Configuration B refers to the arrangement where mass elements are placed at the back end of the interface plate (Fig. 6b). The distance between the two positions of the mass elements is 0.91 m.

During experiments, the rover was commanded to move forward with a constant speed on

soft flat soil, i.e. constant wheel angular velocity of 0.5 rad/s. The wheel encoders confirmed that the wheels operated at the expected angular velocity. A variable, controlled horizontal load was applied to the frame of the rover. The magnitude of this force was adjusted during operation to keep the velocity of the rover within the same range for all the experiments; the value of the force was recorded by a digital load cell. Experimental results were selected from runs where the motor currents were found to be the same for both configurations, so the input power of the system for the two trials can be considered constant between experiments. Under these conditions, the applied load represents the drawbar pull that the rover is able to carry for a given value of input power, for each configuration.

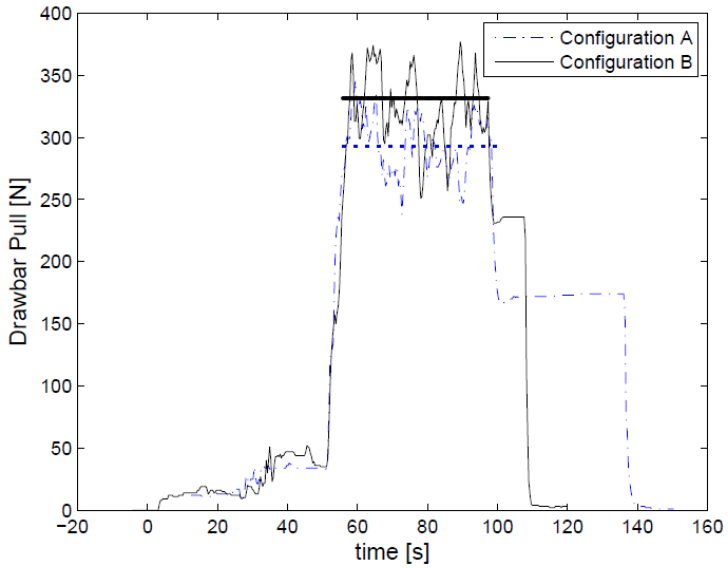

Figure 8: Time history of the loads applied to the rover in experiments with configurations A and B. The average values of the loads during the representative period of the motion are superimposed on the figure as straight lines

As an example, Fig. 8 shows the time history of the force measured by the load cell obtained during two experiments, with configurations A and B. The difference in normal forces between front and rear axes was determined using Eqs. (24) and (25) of the observative model and found to be 1571.6 N with configuration A. For configuration B the difference between normal force components was reduced to 812.3 N. The average value of the applied force was determined for each case based on the digital load cell measurement, as shown in Fig. 8 with horizontal straight lines. For configuration A, the rover was able to develop an average drawbar-pull force close to 290 N (represented in Fig. 8 with a dashed line); for configuration B that value increased to approximately 340 N (represented by a solid line in the figure). These values show that configuration B is more suitable for development of higher traction, or equivalently, for developing higher drawbar pull. The results from experiments with the Juno rover follow the

trend predicted by the simulation results shown in Fig. 7.

The experimental results showed that an uneven distribution of normal forces results in different traction forces developed at each wheel. The kinematic relation between the angular velocities of the two wheels on each side of this rover enforces the same slip at each wheel-terrain contact. The traction force is a function of normal force and slip; for the same value of slip, a smaller normal force provides a lower traction force, although this relation is not linear. If it were, the tangential force in Fig. 7 would be constant, regardless of the normal force distribution. However, in this figure it can be appreciated that the summation of tangential forces in the system reaches its maximum when the two tangential force components are equal due to the balancing of the normal force distribution. The experimental results support this statement, which confirms that the distribution of normal forces can be used as a performance indicator for improving the vehicle mobility. This type of indicators helps us find the configuration which provides higher drawbar pull without the need to go thorough detailed computation of terrain reactions, even though they do not provide the exact value of that drawbar pull. This is a key idea behind the use of observative models.

6 Conclusions

The performance analysis of rovers operating on unstructured terrain can be investigated using performance indicators based on different possible models. We particularly looked at the possibility of applying what we term observative models for the analysis. A central idea of the proposed approach is to model the vehicle-terrain interaction with representative, desired kinematic specifications, and use the resulting constraint reactions as primary variables to evaluate the effect of system parameter changes on the dynamics behaviour and performance. As shown in this paper, such models can capture the effect of changes in system parameters on the dynamic behaviour. Observative models can be used to streamline the design and operation of planetary exploration vehicles. These can have a number of advantages: they are computationally inexpensive, can be used for sensitivity and inverse-dynamics analyses, and can be employed regardless of the properties of the terrain on which the rover operates. They give rise to the possibility of developing performance indicators as functions of rover parameters and state. The resulting constraint reactions are complementary to the motion restricted by the kinematic specifications.

It was shown that tangential and normal forces defined via such models can be used as performance indicators of a rover, thereby obviating the detailed parameterization of the soil.

The performance indicators defined using the observative modelling approach were compared to the results obtained with the predictive forward-dynamics simulations using terramechanics relations. They were also validated against experimental results using a rover prototype. Results showed that the reaction forces associated with both the no-slip and no-penetration conditions can be meaningful indicators for design and operation analyses. Tangential forces can be used to assess how a change in the system parameters can influence the development of slip. Normal force distribution obtained based on the observative approach was used to investigate different inertia distributions of the experimental rover prototype to increase its ability to develop traction and drawbar pull.

Acknowledgments

The research work reported here was supported by the Natural Sciences and Engineering Research Council of Canada, CM Labs Simulations Inc., MacDonald, Dettwiler and Associates (MDA), and the Canadian Space Agency. This support is gratefully acknowledged.

A Appendix

Equations (22)–(25) in Subsection 4.2 provide the expression of the constraint reaction forces associated with the kinematic constraints imposed on the observative model as a function of the desired acceleration $\ddot{x}_G$ of the vehicle, when it moves on flat terrain. The details of their derivation are provided below.

The dynamic equations of the five-dof model of the rover are given by Eq. (1), with $\mathbf{q} = [x_G, y_G, \psi, \phi_1, \phi_2]^{\mathrm{T}}$. The term of generalized forces can be further expanded into its three components, the dynamics equations thus reading

$$\mathbf{M}\ddot{\mathbf{q}} + \mathbf{c} = \mathbf{f}_w + \mathbf{f}_d + \mathbf{f}_o \tag{A.1}$$

The mass matrix of the system is

$$\mathbf{M} = \begin{bmatrix} M_{11} & 0 & M_{13} & 0 & 0 \\ 0 & M_{22} & M_{23} & 0 & 0 \\ M_{31} & M_{32} & M_{33} & M_{34} & M_{35} \\ 0 & 0 & M_{43} & M_{44} & 0 \\ 0 & 0 & M_{53} & 0 & M_{55} \end{bmatrix} \tag{A.2}$$

with

$$\begin{aligned} &M_{11} = M_{22} = \ m_b + 2m_w, \quad M_{13} = M_{31} = \ m_w \left((b_2 - b_1) \ \sin\psi + 2h\cos\psi \right) \\ &M_{23} = M_{32} = \ m_w \left((b_1 - b_2) \ \cos\psi + 2h\sin\psi \right), \quad M_{33} = \ m_w \left(b_1^2 + b_2^2 + 2h^2 \right) + I_b + 2I_w \\ &M_{34} = M_{43} = \ I_w, \quad M_{35} = M_{53} = \ I_w, \quad M_{44} = M_{55} = \ I_w \end{aligned} \tag{A.3}$$

while the Coriolis and centrifugal terms are

$$\mathbf{c} = \begin{bmatrix} \dot{\psi}^2 m_w \left((b_2 - b_1) \ \cos\psi - 2h\sin\psi \right), \dot{\psi}^2 m_w \left((b_2 - b_1) \ \sin\psi + 2h\cos\psi \right), 0, 0, 0 \end{bmatrix}^{\mathrm{T}} \tag{A.4}$$

where the masses of the wheels have been assigned as $m_1 = m_2 = m_w$, their moments of inertia as $I_1 = I_2 = I_w$.

The last two components of the generalized forces are given below:

$$\mathbf{f}_d = [0, 0, 0, T_1, \alpha T_1]^{\mathrm{T}} \tag{A.5}$$

$$\mathbf{f}_o = [0, m_b g + 2m_w g, m_w g \left(b_1 \cos\psi - b_2 \cos\psi + 2h\sin\psi \right), 0, 0]^{\mathrm{T}} \tag{A.6}$$

The kinematic relations imposing no-slip and no-penetration used in the definition of the observative model are given below. The no-slip condition on flat terrain is

$$\begin{cases} \dot{\phi}_1 = \dot{x}_G / r_1 \\ \dot{\phi}_2 = \dot{x}_G / r_2 \end{cases} \Rightarrow \begin{cases} \ddot{\phi}_1 = \ddot{x}_G / r_1 \\ \ddot{\phi}_2 = \ddot{x}_G / r_2 \end{cases} \tag{A.7}$$

Similarly, for the no-penetration condition we have

$$\begin{cases} \dot{y}_G = 0 \\ \dot{\psi} = 0 \end{cases} \Rightarrow \begin{cases} \ddot{y}_G = 0 \\ \ddot{\psi} = 0 \end{cases} \tag{A.8}$$

The imposition of these four kinematic constraints reduces the number of degrees of freedom of the system to one. In this case, the motion of the system can be fully determined upon specifying the acceleration $\ddot{x}_G$ of the rover . The reaction forces for the no-slip and no-penetration constraints are the tangential (λ_{ui}) and normal (λ_{vi}) reactions on each wheel-ground contact point. These unknown reaction forces and the required applied torque are now grouped in an array $\boldsymbol{\lambda} = [\lambda_{u1}, \lambda_{u2}, \lambda_{v1}, \lambda_{v2}, T_1]^{\mathrm{T}}$. Reordering Eq. (A.1) as

$$\mathbf{f}_w + \mathbf{f}_d = \mathbf{M}\ddot{\mathbf{q}} + \mathbf{c} - \mathbf{f}_o \tag{A.9}$$

leaves all the unknown terms on the left hand side, while the right hand side is fully known. In order to find $\boldsymbol{\lambda}$, a transformation from array $\mathbf{a} = \mathbf{f}_w + \mathbf{f}_d$ can be used.

The virtual work of the unknown forces is

$$\begin{aligned} \delta W = {} & \lambda_{u1} \left(\delta x - \delta\psi \left(b_1 \sin\psi - h\cos\psi\right) + \left(\delta\psi + \delta\phi_1\right) r_1\right) \\ & + \lambda_{u2} \left(\delta x - \delta\psi \left(-b_2 \sin\psi - h\cos\psi\right) + \left(\delta\psi + \delta\phi_2\right) r_2\right) \\ & + \lambda_{v1} \left(\delta y + \delta\psi \left(b_1 \cos\psi + h\sin\psi\right)\right) + \lambda_{v2} \left(\delta y + \delta\psi \left(-b_2 \cos\psi + h\sin\psi\right)\right) \\ & + T_1\delta\phi_1 + \alpha T_1 \delta\phi_2 \end{aligned} \tag{A.10}$$

while the corresponding term in the dynamics equations is

$$\mathbf{a} = \mathbf{f}_w + \mathbf{f}_d = \frac{\partial \delta W}{\partial \delta \mathbf{q}} = \begin{bmatrix} a_1 & a_2 & a_3 & a_4 & a_5 \end{bmatrix}^{\mathrm{T}} \tag{A.11}$$

with

$$\begin{aligned} a_1 = {} & \lambda_{u1} + \lambda_{u2}; \quad a_2 = \lambda_{v1} + \lambda_{v2} \\ a_3 = {} & \lambda_{u1} \left(h\cos\psi - b_1 \sin\psi + r_1\right) + \lambda_{v1} \left(b_1 \cos\psi + h\sin\psi\right) \\ & + \lambda_{u2} \left(b_2 \sin\psi + h\cos\psi + r_2\right) + \lambda_{v2} \left(h\sin\psi - b_2 \cos\psi\right) \\ a_4 = {} & \lambda_{u1} r_1 + T_1; \quad a_5 = \lambda_{u2}\, r_2 + \alpha T_1 \end{aligned} \tag{A.12}$$

It is possible to relate $\mathbf{a}$ and $\boldsymbol{\lambda}$ with a velocity transformation $\mathbf{v} = \mathbf{J}\dot{\mathbf{q}}$, where $\mathbf{v}$ contains the velocities of the application points of forces $\boldsymbol{\lambda}$. Matrix $\mathbf{J}$ is

$$\mathbf{J} = \begin{bmatrix} 1 & 0 & h\cos\psi - b_1\sin\psi + r_1 & r_1 & 0 \\ 1 & 0 & b_2\sin\psi + h\cos\psi + r_2 & 0 & r_2 \\ 0 & 1 & b_1\cos\psi + h\sin\psi & 0 & 0 \\ 0 & 1 & -b_2\cos\psi + h\sin\psi & 0 & 0 \\ 0 & 0 & 0 & 1 & \alpha \end{bmatrix} \tag{A.13}$$

In this case, $\mathbf{J}$ is non-singular, the relation between the two sets of forces then being

$$\boldsymbol{\lambda} = \mathbf{J}^{-\mathrm{T}}\mathbf{a} \tag{A.14}$$

and Eq. (A.14) can be substituted into Eq. (A.9), which yields the expression of the unknown forces

$$\boldsymbol{\lambda} = \mathbf{J}^{-\mathrm{T}}\left(\mathbf{M}\ddot{\mathbf{q}} + \mathbf{c} - \mathbf{f}_o\right) \tag{A.15}$$

Finally, imposing constraint equations (A.7) and (A.8) onto Eq. (A.15), and setting $\psi = 0$, $r_1 = r_2 = r$, and $h_1 = h_2 = h$ yields the parametric expression of the reaction forces and the applied torque:

$$\lambda_{u1} = \frac{1}{\alpha+1}\left[m_b + 2m_w - \frac{\alpha I_w}{r^2} + \frac{I_w}{r^2}\right]\ddot{x}_G \tag{A.16}$$

$$\lambda_{u2} = \frac{1}{\alpha+1}\left[\alpha\left(m_b + 2m_w\right) + \frac{\alpha I_w}{r^2} - \frac{I_w}{r^2}\right]\ddot{x}_G \tag{A.17}$$

$$\lambda_{v1} = \frac{1}{b_1+b_2}\left[-\left(m_b h + 2m_w r + m_b r\right)\ddot{x}_G - m_w g\left(b_1+b_2\right) - m_b g b_2 - 2\frac{I_w}{r}\ddot{x}_G\right] \tag{A.18}$$

$$\lambda_{v2} = \frac{1}{b_1+b_2}\left[\left(m_b h + 2m_w r + m_b r\right)\ddot{x}_G - m_w g\left(b_1+b_2\right) - m_b g b_2 + 2\frac{I_w}{r}\ddot{x}_G\right] \tag{A.19}$$

$$T_1 = \frac{-r}{\alpha+1}\left(m_b + 2m_w + \frac{2I_w}{r^2}\right)\ddot{x}_G \tag{A.20}$$

References

[1] Apostolopoulos, D.: Analytical configuration of wheeled robotic locomotion. Ph.D. thesis, Carnegie Mellon University (2001)

[2] Azimi, A.: Wheel-soil interaction modelling for rover simulation and analysis. Ph.D. thesis, Department of Mechanical Engineering, McGill University (2013)

[3] Azimi, A., Hirschkorn, M., Ghotbi, B., Kövecses, J., Angeles, J., Radziszewski, P., Teichmann, M., Courchesne, M., Gonthier, Y.: Terrain modelling in simulation-based performance evaluation of rovers. Canadian Aeronautics and Space Journal **57**(1), 24–33 (2011). DOI 10.5589/q11-005

[4] Azimi, A., Kövecses, J., Angeles, J.: Wheel-soil interaction model for rover simulation and analysis using elastoplasticity theory. IEEE Transactions on Robotics **29**(5), 1271–1288 (2013). DOI 10.1109/TRO.2013.2267972

[5] Bauer, R., Barfoot, T., Leung, W., Ravindran, G.: Dynamic simulation tool development for planetary rovers. International Journal of Advanced Robotic Systems **5**(3), 311–314 (2008)

[6] Bekker, M.G.: Introduction to Terrain-Vehicle Systems. The University of Michigan Press, Ann Arbor (1969)

[7] Campion, G., Bastin, G., D'Andréa-Novel, B.: Structural properties and classification of kinematic and dynamic models of wheeled mobile robots. IEEE Transactions on Robotics and Automation **12**(1), 47–62 (1996). DOI 10.1109/70.481750

[8] Contreras, U., Li, G., Foster, C.D., Shabana, A.A., Jayakumar, P., Letherwood, M.D.: Soil models survey and vehicle system dynamics. In: Proceedings of the ASME 2012 International Design Engineering Technical Conferences & Computers and Information in Engineering Conference IDETC/CIE, DETC2012-71450, pp. 623–640. Chicago, IL, USA (2012)

[9] Ding, L., Deng, Z., Gao, H., Nagatani, K., Yoshida, K.: Planetary rovers' wheel–soil interaction mechanics: New challenges and applications for wheeled mobile robots. Intelligent Service Robotics **4**(1), 17–38 (2011). DOI 10.1007/s11370-010-0080-5

[10] Ghotbi, B., Azimi, A., Kövecses, J., Angeles, J.: Sensitivity analysis of mobile robots for unstructured environments. In: Proceedings of the ASME 2011 International Design Engi-

neering Technical Conferences & Computers and Information in Engineering Conference IDTC/CIE 2011, DETC2011-48440, pp. 641–647. Washington, DC (2011)

[11] Ghotbi, B., González, F., Kövecses, J., Angeles, J.: Vehicle-terrain interaction models for analysis and performance evaluation of wheeled rovers. In: Proceedings of the 2012 IEEE/RSJ International Conference on Intelligent Robots and Systems IROS 2012, pp. 3138–3143. Vilamoura, Portugal (2012). DOI 10.1109/IROS.2012.6386208

[12] González, F., Kövecses, J.: Use of penalty formulations in dynamic simulation and analysis of redundantly constrained multibody systems. Multibody System Dynamics **29**, 57–76 (2013). DOI 10.1007/s11044-012-9322-y

[13] Iagnemma, K., Dubowsky, S.: Traction control of wheeled robotic vehicles in rough terrain with application to planetary rovers. The International Journal of Robotics Research **23**(10-11), 1029–1040 (2004). DOI 10.1177/0278364904047392

[14] Iagnemma, K., Kang, S., Shibly, H., Dubowsky, S.: Online terrain parameter estimation for wheeled mobile robots with application to planetary rovers. IEEE Transactions on Robotics **20**(5), 921 – 927 (2004). DOI 10.1109/TRO.2004.829462

[15] Iagnemma, K., Rzepniewski, A., Dubowsky, S., Pirjanian, P., Huntsberger, T., Schenker, P.: Mobile robot kinematic reconfigurability for rough-terrain. In: Proceedings of the SPIE Symposium on Sensor Fusion and Decentralized Control in Robotic Systems III, vol. 4196 (2000). DOI 10.1117/12.403739

[16] Iagnemma, K., Senatore, C., Trease, B., Arvidson, R., Bennett, K., Shaw, A., Zhou, F., Van Dyke, L., Lindemann, R.: Terramechanics modeling of Mars surface exploration rovers for simulation and parameter estimation. In: Proceedings of the ASME 2011 International Design Engineering Technical Conferences & Computers and Information in Engineering Conference, DETC2011-48770, pp. 805–812. Washington, DC, USA (2011)

[17] Ishigami, G., Miwa, A., Nagatani, K., Yoshida, K.: Terramechanics-based model for steering maneuver of planetary exploration rovers on loose soil. Journal of Field Robotics **24**(3), 233–250 (2007). DOI 10.1002/rob.20187

[18] Jain, A., Guineau, J., Lim, C., Lincoln, W., Pomerantz, M., Sohl, G., Steele, R.: ROAMS: Planetary surface rover simulation environment. In: Proceedings of the 7th International Symposium on Artificial Intelligence, Robotics and Automation in Space: i-SAIRAS 2003. Nara, Japan (2003)

[19] Lamon, P., Krebs, A., Lauria, M., Siegwart, R., Shooter, S.: Wheel torque control for a rough terrain rover. In: Proceedings of the 2004 IEEE International Conference on Robotics and Automation, ICRA 2004, vol. 5, pp. 4682 – 4687. New Orleans, LA, USA (2004). DOI 10.1109/ROBOT.2004.1302456

[20] Patel, N., Slade, R., Clemmet, J.: The ExoMars rover locomotion subsystem. Journal of Terramechanics **47**(4), 227–242 (2010). DOI 10.1016/j.jterra.2010.02.004

[21] Sreenivasan, S., Wilcox, B.: Stability and traction control of an actively actuated micro-rover. Journal of Robotic Systems **11**(6), 487–502 (1994). DOI 10.1002/rob.4620110604

[22] Thueer, T., Krebs, A., Siegwart, R., Lamon, P.: Performance comparison of rough-terrain robots – simulation and hardware. Journal of Field Robotics **24**(3), 251–271 (2007). DOI 10.1002/rob.20185

[23] Thueer, T., Siegwart, R.: Mobility evaluation of wheeled all-terrain robots. Robotics and Autonomous Systems **58**(5), 508–519 (2010). DOI 10.1016/j.robot.2010.01.007

[24] Wong, J.Y.: Theory of Ground Vehicles, fourth edn. John Wiley & Sons, Inc, New Jersey (2008)